Upper Critical Solution Temperature Behavior of pH-Responsive Amphoteric Statistical Copolymers in Aqueous Solutions

Komol Kanta Sharker, Yusuke Shigeta, Shinji Ozoe, Panittha Damsongsang, Voravee P. Hoven, and Shin-ichi Yusa*

ACCESS | Metrics & More | Article Recommendations | Supporting Information

ABSTRACT: Amphoteric statistical equivalent copolymers $(P(2VP/NaSS)_n)$ composed of 2-vinylpyridine (2VP) and anionic sodium p-styrenesulfonate (NaSS) were prepared via reversible addition−fragmentation chain transfer polymerization. The degrees of polymerization (n) were 19 and 95. The monomer reactivity ratio, time conversion profile, and ^{1}H nuclear magnetic resonance diffusion-ordered spectra suggested that the copolymerization of 2VP and NaSS provided statistical or near to random copolymers. $P(2VP/NaSS)_n$ exhibited an upper critical solution temperature (UCST) in acidic aqueous solutions on the basis of the charge interactions between the protonated cationic 2VP and anionic NaSS units. With an increase in pH value, the interaction was weakened because of the deprotonation of the 2VP units, thus reducing the UCST. At high [NaCl], the electrostatic interactions among the polymers were weakened because of the screening effect, and again, the UCST was reduced. With an increase in polymer concentration, the intra- and interpolymer interactions increased because of some entanglement, and the UCST consequently increased. Electrostatic interactions among the polymer chains with high molecular weight occurred easier than those among the low-molecular-weight polymer chains, which increased the UCST. The UCST also increased when deuterium oxide was used instead of hydrogen oxide, which was due to the isotopic effect. Hence, the UCST of $P(2VP/NaSS)_n$ can be adjusted according to the desired application.
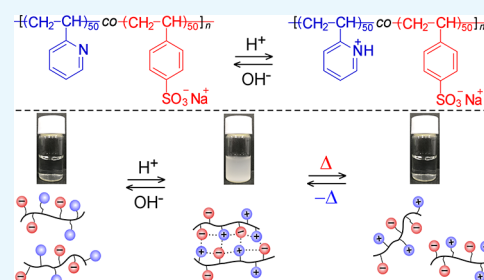
INTRODUCTION

Polymers that change their physical or chemical properties by responding to their surrounding environment are known as "stimuli-responsive" or "smart" polymers. These environmental changes include temperature,[1] pH,[2] ionic strength,[3] light,[4] electric and magnetic fields,[5,6] or a combination of each.[7] By responding to the stimuli, these polymers change their conformation, morphology, solubility, and molecular assembly, which generally involves a change in the molecular interactions, hydrophilic−hydrophobic balance in the materials, or energy variation. Among the stimuli-responsive polymers, thermo-responsive polymers are the most studied because of the easy control of the temperature. Thermo-responsive polymers change their properties when experiencing heating or cooling. The ability of these polymers to change their properties via temperature changes is highly desirable from the viewpoint of their desired applications. Since their properties can be tuned according to the demand, thermo-responsive polymers are widely used in various fields, including drug release,[8,9] gene therapy,[10] bio-separation,[11] thermally switchable optical devices,[12] bio-imaging,[13] and catalysis.[14] Besides the single-stimulus type, multiple stimuli-responsive (e.g., temperature and pH[15,16]) polymers can also widen the application scope. Various pH-responsive groups, such as carboxyl, pyridine, phosphate, and tertiary amine groups, are incorporated to achieve a pH-responsive property. The

characteristics of the pH-responsive behavior in combination with the thermo-responsive behavior promote the numerous applications of the polymers in the broader fields of science and technology.[17,18]

Thermo-responsive polymers can be divided into two classes, namely, lower critical solution temperature (LCST) and upper critical solution temperature (UCST) polymers, where the miscibility gap is observed at high and low temperatures, respectively. The LCST and UCST polymers have been studied by various research groups over the past few decades. In 1968, Guillet and Heskins[19] were the first to report an LCST polymer, poly(N-isopropylacrylamide) (PNIPAM), in water. Since then, PNIPAM has become the most studied thermo-responsive polymer because of its phase transition near physiological temperatures of 32 °C. The phase transition between body temperature and room temperature is important in medical applications.[20] To increase the application scope, various other LCST-type water-soluble polymers, including poly(2-oxazoline)s,[21] poly(N-vinyl caprolactam),[22] poly(oligo-

(ethylene glycol) methacrylate),[23] poly(2-(N,N-diethylamino)-ethyl acrylamide),[24] and poly(2-(N,N-dimethylamino)ethyl methacrylate),[25] have been discovered.

Meanwhile, UCST water-soluble polymers have not been so well documented, although they are as equally useful as LCST polymers. This may be due to the major challenges in preparing this type of polymer. Here, appropriate tuning in terms of interpolymer attraction and hydrophilicity of the polymer is required. However, UCST polymers offer numerous advantages in biological science in terms of autoregulated drug delivery when the body temperature is increased as well as in various other fields.[26] Thus, researchers have begun to turn their attention to developing UCST-type polymers and to investigate their full application scope. Up to this point, poly(sulfobetaine)[27] and poly(acrylic acid) and poly-(acrylamide)[28,29] are the most studied UCST polymers, all of which exhibit a phase transition in water under workable conditions. The UCST polymer in water can be divided into two main types, namely, polymers with anion and cation interactions, which are known as zwitterionic polymers,[27] and hydrogen-bonded polymers.[30] Schulz et al.[31] reported a poly(N-(3-sulfopropyl)-N-methacroyloxyethyl-N,N-dimethyl-lammonium betaine) polymer that exhibited UCST behavior because of the charge interactions. Following this, various research groups have studied other ionic UCST polymers.[32−35] Here, Agarwal and Seuring[30] demonstrated a poly(N-acryloyl glycinamide) polymer that exhibited UCST behavior due to the hydrogen bonding interactions as well as various non-ionic UCST polymers, before extending their research using acrylamide (AAm) with another comonomer, such as styrene or acrylonitrile.[36,37] However, the application of these polymers is hindered by various limitations. For one, the chemical stability of the polymers is not sufficient since AAm and N-acryloyl glycinamide tend to hydrolyze. A small amount of ionic group substance generated as a result of hydrolysis during polymerization can hinder the polymer's capacity to exhibit UCST behavior, whereas the ionic group generated from the initiator or monomer can bring some impurity to the system.[38] Poly(sulfobetaine) is well suited to a system containing salts, i.e., in a physiological environment with a tunable UCST value, despite its higher molar mass. The concept of charge interactions has encouraged researchers to focus on the development of polyampholytes. Here, Zhang and Hoogenboom[26] reported the synthesis of polyampholytes from methacrylic acid and 2-(N,N-dimethylamino)ethyl methacry-late via reversible addition−fragmentation chain transfer (RAFT) copolymerization. The resulting polymer exhibited a UCST-type phase transition in an alcohol/water mixture, which would limit its applications in certain cases. This prompted the search for a new copolymer that exhibits UCST behavior in pure water as well as under physiological conditions. The development of several controlled polymer-ization techniques, including group transfer polymerization, atom transfer radical polymerization, nitroxide-mediated radical polymerization, and RAFT, has facilitated the synthesis of polymers with well-defined structures.[39]

A controlled polymer structure is often the prerequisite for achieving certain special properties that cannot be obtained from an uncontrolled polymer structure. Moreover, copoly-merization, e.g., statistical, random, gradient, block, graft, and star, can be used to manipulate the properties of the polymer.[40] Here, Varoqui et al.[41] prepared a diblock copolymer composed of poly(sodium styrenesulfonate) (PNaSS) and poly(2-vinyl-pyridine) (P2VP) via anionic polymerization and focused on the polyelectrolyte behavior of this polyampholyte, that is, the electrochemical characteristics of the basic P2VP in the presence of the neighboring PNaSS chain. The degree of ionization of P2VP in the diblock copolymer was studied as a function of pH, with the phase separation of the polymer solution found to occur at a pH of <2.5. Also, some amphoteric copolymers were prepared via RAFT polymerization; however they did not report the thermo-responsive behavior of the amphoteric copolymers.[42,43] In our previous study, we prepared an amphoteric statistical copolymer from cationic vinylbenzyl trimethylammonium chloride and anionic sodium p-styrenesulfonate (NaSS) via a controlled RAFT method to reveal the UCST thermo-responsivity in aqueous solutions due to the charge interactions.[32]

In the present study, we prepared statistical poly(2-vinylpyridine-co-sodium p-styrenesulfonate) (P(2VP/NaSS)$_n$) composed of pH-responsive cationic 2VP and anionic NaSS via RAFT polymerization (Scheme 1). The abbreviation n in

Scheme 1. Chemical Structures of the Statistical Copolymer, P(2VP/NaSS)$_n$, in Acidic Form


P(2VP/NaSS50)$_n$ n = 19 and 95

P(2VP/NaSS)$_n$ represents the degrees of polymerization (DP), which were 19 and 95. Under acidic conditions, the 2VP unit became protonated, whereas electrostatic attraction occurred with the anionic NaSS unit. Meanwhile, P(2VP/NaSS)$_n$ exhibited UCST behavior in aqueous solutions because of the charge interactions, whereas pH, molar mass, NaCl concentration, polymer concentration, and deuterium isotope were found to affect the UCST behavior. The UCST value decreased with an increase in pH and NaCl concentration and a reduction in polymer concentration and molar mass. The UCST in deuterium oxide (D$_2$O) was higher than that in hydrogen oxide (H$_2$O) because of the isotropic effect. Hence, tunable dual pH- and thermo-responsive behavior of P(2VP/NaSS)$_n$ could open new doors for applications in various fields.

■ RESULTS AND DISCUSSION

The controlled synthesis of P(2VP/NaSS)$_n$ with n = 19 and 95 was performed using pH-responsive cationic 2VP and anionic NaSS via RAFT polymerization (Scheme 1).

We studied the relationship between the polymerization time and the individual monomer conversion (p) of 2VP and NaSS as well as their kinetics in a mixed solvent of D$_2$O and methanol-d_4 (9/1, v/v) when 2VP and NaSS were equimolarly copolymerized (Figure 1). The reaction was performed using NMR equipment under an argon atmosphere at 70 °C. The p value of 2VP was estimated from the average integral intensity of the vinyl peak at 5.3 and 5.9 ppm, whereas for NaSS, this value was determined from the average integral intensity of the vinyl peak that appeared at 5.0 and 5.6 ppm before and after polymerization. There was no polymerization within the first 5 min of the process. This is generally termed as the induction period, which is a common phenomenon in the RAFT process.[44,45] At the initial stages of polymerization for 2VP and
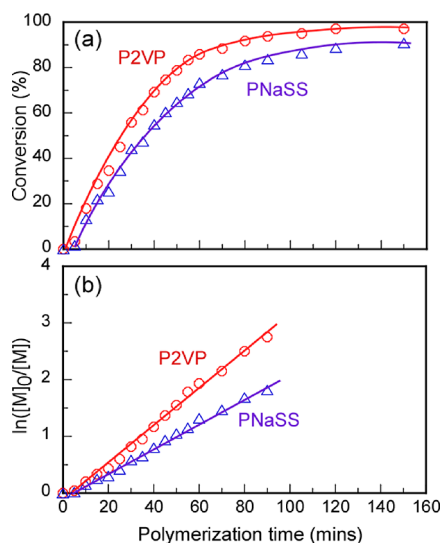
Figure 1. (a) Time conversion and (b) first-order kinetic plots for pH-responsive cationic 2VP (open red circle) and anionic NaSS (open violet triangle) for RAFT copolymerization in a mixed solvent of D_2O and methanol-d_4 (9/1 = v/v) at 70 °C performed using NMR equipment.

following the induction period for NaSS, the first-order kinetic plot increased linearly with an increase in conversion up to 90 min, indicating that the growth of propagating radicals remained constant in this period. The reaction was terminated when the 2VP conversion reached 97.2% at 150 min. Within this period, the conversion of NaSS reached 91.0%. This suggests that the copolymer prepared using the two monomers contained a higher mole fraction of 2VP, although they were equimolarly copolymerized, which was due to the higher reactivity ratio of 2VP compared with NaSS. The first-order kinetic plots also support this (Figure 1b).

We wanted to ascertain whether the 2VP and NaSS monomer pairs were alternatively, randomly, or statistically copolymerized. One effective way to understand the nature of the copolymerization of a monomer pair involves determining the reactivity ratio. The nature of the copolymerization of the 2VP and NaSS monomer pairs was thus investigated when polymerized, with their reactivity ratios determined via conventional free-radical polymerization in a mixed solvent of D_2O/methanol-d_4 (7/3; v/v) at 70 °C. A <15% conversion was performed to determine the reactivity ratio at varying 2VP molar feed ratios. As the reaction proceeded, there was the possibility of a shift in the composition of the monomer feed. To avoid this bias of composition, reactions were conducted at a low conversion level.[46,47] The conversion of 2VP was estimated from the average integral intensity ratio of the intensity peak at 5.3 and 5.9 ppm before and after polymerization. Figure 2a shows the relationship between the 2VP content in the feed and in the copolymer. The ratio ($m_{2VP}/m_{NaSS} = f$) of the contents of 2VP and NaSS in the copolymer obtained via random copolymerization can be represented by the following copolymer equation:

$$\frac{m_{2VP}}{m_{NaSS}} = \frac{[M_{2VP}]}{[M_{NaSS}]} \times \frac{r_{2VP}[M_{2VP}] + [M_{NaSS}]}{r_{NaSS}[M_{NaSS}] + [M_{2VP}]} \quad (1)$$

where m_{2VP} and m_{NaSS} are the molar contents of 2VP and NaSS in the random copolymer, $[M_{2VP}]$ and $[M_{NaSS}]$ are the molar concentrations of 2VP and NaSS monomers, respec-
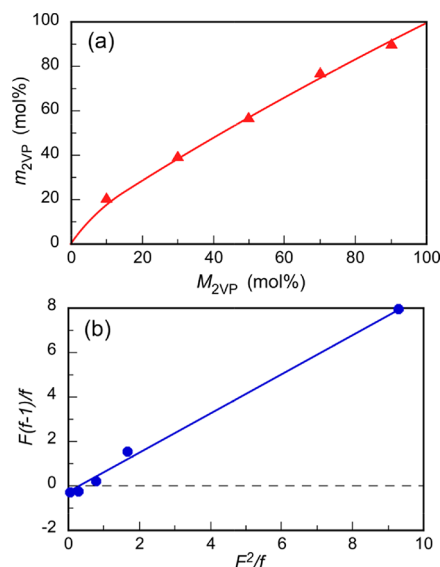
Figure 2. (a) Relationship between the 2VP content in the copolymer (m_{2VP}) and the feed (M_{2VP}). (b) Relationship between $F(f-1)/f$ and F^2/f, where $f = m_{2VP}/m_{NaSS}$ and $F = M_{2VP}/M_{NaSS}$; m_{NaSS} and M_{NaSS} are the molar contents of NaSS in the copolymer and the feed, respectively.

tively, before polymerization, and r_{2VP} and r_{NaSS} are the monomer reactivity ratios of 2VP and NaSS, respectively. Then, eq 1 can be rewritten in terms of the Fineman−Ross equation:

$$\frac{F(f-1)}{f} = \frac{r_{NaSS}F^2}{f - r_{2VP}} \quad (2)$$

where $F = M_{2VP}/M_{NaSS}$ and $f = m_{2VP}/m_{NaSS}$. A Fineman−Ross plot was prepared based on eq 2, as shown in Figure 2b.[48] The r_{2VP} and r_{NaSS} were estimated from the slope and intercept, with the values found to be 0.897 and 0.329, respectively.

Copolymerization with $r_1 \times r_2 \ll 1$ or $r_1 \times r_2 = 0$ generally favors alternating copolymerization.[49] When r_1 and r_2, which are the monomer reactivity ratios of monomer 1 and 2, respectively, are close to 1, the monomer units are randomly distributed in the copolymer, i.e., $r_1 \times r_2 = 1$.[50] Hence, the obtained copolymers may be statistical or near to random. The reactivity of the 2VP monomer was 2.7 times higher than that of the NaSS monomer. Therefore, the NaSS monomer was less reactive in terms of adding its own unit to the growing chain than 2VP. As such, the copolymer contained a higher molar content of 2VP than NaSS.

The nature of the copolymerization can be predicted based on the interaction occurring between the monomer pairs. Monomers tend to form a complex before participating in the alternative copolymerization.[51] Salamone et al.[52] also noted that the charge-transfer interaction between the monomers is the prerequisite to yielding alternative copolymers. Here, the authors demonstrated that a 4-vinylpydinium chloride and NaSS charge-transfer complex is formed through the interaction between the electron-withdrawing pyridinium group and the electron-donating NaSS, which leads to the formation of alternative copolymers. We investigated the complex formation of 2VP and NaSS before copolymerization in the polymerization solvent at room temperature. Here, ^1H NMR DOSY measurements were performed to investigate the diffusion coefficient (D) of the individual monomer and the

Table 1. Monomer Conversion (p), Composition, DP, M_n, and T_p for the Statistical Copolymers

samples	p^a (%)	NaSS in feed (mol %)	NaSS content^b (mol %)	DP (theory)^c	M_n(theory)^d ($\times 10^3$ g/mol)	T_p (°C)^e
P(2VP/NaSS)$_{19}$	94.1	50	47.5 ± 0.8	19	2.97	52.4
P(2VP/NaSS)$_{95}$	95.2	50	48.2 ± 1.0	95	15.12	72.5

^{a}Estimated from ^{1}H NMR after polymerization. ^{b}Based on ^{1}H NMR. ^{c}Estimated from eq 3. ^{d}Estimated from eq 4. $^e T_p$ upon cooling for 0.1 M NaCl aqueous P(2VP/NaSS)$_{19}$ solution and 1.2 M NaCl aqueous P(2VP/NaSS)$_{95}$ solution at pH = 2 and C_p = 2.0 g/L.

mixed equimolar monomer solution. If a complex is formed between 2VP and NaSS, the D values for both monomers in the mixed monomer solution should be both the same and much lower than their individual values. Figure S1 shows the DOSY measurement and the corresponding 2D DOSY data for the individual and mixed monomer solutions. NaSS is soluble in pure water, whereas the solubility of 2VP is limited. However, this solubility is increased in the presence of NaSS. Hence, we could not measure the diffusion for the individual 2VP monomer because of its lower solubility. Thus, we estimated the D value for the individual NaSS monomer solution and the 2VP/NaSS monomer equimolar mixed solution. The D value obtained for the individual NaSS was 4.1×10^{-10} m^2 s^{-1}, whereas in the case of the 2VP/NaSS mixture, the D values for 2VP and NaSS were both 2.8×10^{-10} m^2 s^{-1}. Besides being the same, the D values for both monomers in the mixed monomer solution were also lower than that for the individual NaSS monomer, which indicated the presence of a slight interaction between the monomers. Therefore, there is a trend for this type of monomer pair to copolymerize randomly to alternatively under these polymerization conditions. Moreover, we used noncharged 2VP, which has an electron-donating nature. Therefore, there was a slight chance of forming a charge-transfer complex of 2VP with electron-donating NaSS. Also, in all cases of polymerization, the solution pH was slightly acidic but above the pK_a value of 2VP (4.98). This depicts that, there is a little or no chance of protonation of 2VP and hence absence of ion-paired interactions between 2VP and NaSS. Hence, our synthesized copolymer was neither truly random nor alternative. The UV–vis absorption spectra of the individual monomers, 2VP and NaSS with a 3×10^{-5} M monomer concentration, and their equimolar mixed solution were measured at room temperature in pure water (Figure S2). The absorption spectra for the 2VP monomer were observed at 234 and 278 nm, whereas for the NaSS monomer, the absorption spectra were observed at 198 and 254 nm. For the mixed monomer solution, the absorption spectrum was observed at 242 nm, with the difference clearly indicating interactions between the two monomers.

We estimated the theoretical DP (DP(theory)) and the theoretical molecular weight (M_n(theory)) of the synthesized statistical copolymers via the following formula using the p obtained from the ^{1}H NMR measurement:

$$DP(\text{theory}) = \frac{[M]_0}{[CTA]_0} \times \frac{p}{100} \tag{3}$$

$$M_n(\text{theory}) = DP(\text{theory}) \times M_m + M_{CTA} \tag{4}$$

where $[M]_0$ is the initial monomer concentration, $[CTA]_0$ is the initial chain transfer agent (CTA) concentration, M_m is the molecular weight of the monomer, and M_{CTA} is the molecular weight of CTA. The values of M_n(theory) for P(2VP/NaSS)$_{19}$ and P(2VP/NaSS)$_{95}$ were 2.97×10^3 and 1.51×10^4 g/mol, respectively (Table 1).

Figure S3 shows the IR spectra for P(2VP/NaSS)$_{19}$ and P(2VP/NaSS)$_{95}$, which were highly similar since the solutions had the same composition. The characteristic peaks observed at 2931 and 2856 cm^{-1} were due to the C–H stretching absorption for the aromatic and aliphatic, respectively, whereas the peaks that appeared at 1628 and 1470 cm^{-1} corresponded to the C=C stretching for the aromatic. Meanwhile, the peak at 1595 cm^{-1} was due to the C=N stretching, and that at 416 cm^{-1} was due to the C–N stretching in the pyridine ring, whereas the peak at 1178 cm^{-1} was due to the –SO$_3$ stretching. The peak at 679 cm^{-1} was due to the C–H out-of-plane bending vibration for all,[53] whereas the peak that appeared at 3475 cm^{-1} was due to the stretching of O–H, which may have been induced by the absorption of the water by the polymer.

The ^{1}H NMR spectra for P(2VP/NaSS)$_n$ were measured in D$_2$O at 25 °C (Figure S4). Characteristic peaks due to the main chain protons were observed at 0.8–2.5 ppm. The pendant aromatic protons attributed to the 2VP and NaSS units were overlapped at 5.8–8.5 ppm. By comparing the integral intensities of the pendant aromatic protons in the 2VP units at 5.8–6.7 ppm and in the 2VP and NaSS units at 5.8–7.7 ppm, the NaSS contents were estimated to be around 47.5 ± 0.8 mol % in P(2VP/NaSS)$_{19}$ and 48.2 ± 1.0 mol % in P(2VP/NaSS)$_{95}$, which was similar to the results obtained from the quantitative ^{13}C NMR spectra. Figure 3 shows the
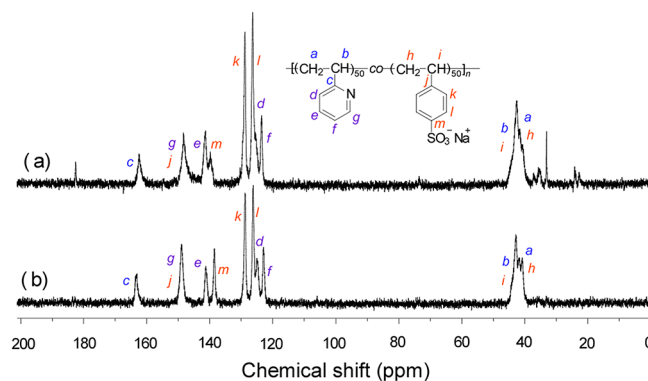

Figure 3. Quantitative ^{13}C NMR spectra for (a) P(2VP/NaSS)$_{19}$ and (b) P(2VP/NaSS)$_{95}$ in D$_2$O at 25 °C.

quantitative ^{13}C NMR spectra for P(2VP/NaSS)$_n$ in D$_2$O at room temperature. The average contents of NaSS were estimated to be 47.2 mol % for P(2VP/NaSS)$_{19}$ and 47.3 mol % for P(2VP/NaSS)$_{95}$, which was achieved by comparing the integrated intensity ratio of peak c appearing at 162 ppm and of peaks g and j appearing at 148 ppm and by comparing the integrated intensity ratio of peak c appearing at 162 ppm and peak m at 139 ppm as well as peak e appearing at 142 ppm and peak k at 128 ppm. The NaSS unit in the copolymer was less than the feed ratio, which was due to the less reactive nature of NaSS compared with 2VP. This finding was also in line with our previous observations.

The nitrogen center of a pyridine ring contains a single pair of electrons. Under acidic conditions, this single pair of electrons forms a N−H bond with the proton of the acid and behaves like a positive ion. Thus, in the presence of an acid pyridine ring, P(2VP/NaSS)$_n$ could be protonated (Scheme 1), and strong electrostatic attraction may occur with an anionic sulfonate group. In our previous study, we demonstrated that polyampholytes prepared from cationic vinylbenzyl trimethylammonium chloride and anionic NaSS exhibit UCST phase transition behavior due to the electrostatic attraction between the cationic and anionic charged group in pure water and in NaCl aqueous solutions.[54] Hence, we expected a UCST phase transition of P(2VP/NaSS)$_n$ under acidic conditions.

Figure 4 shows the %T under various pH conditions for P(2VP/NaSS)$_n$ in water and in the 0.1 M NaCl aqueous
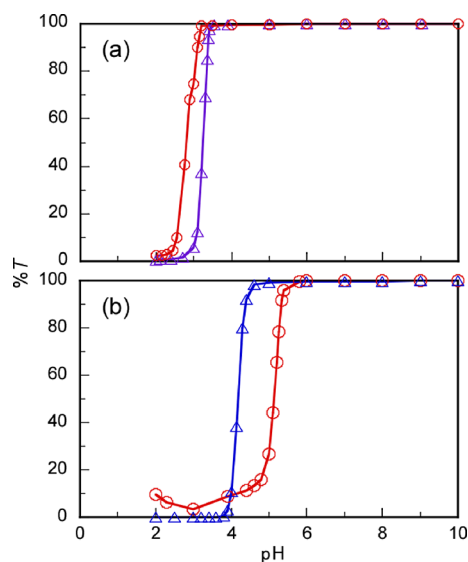

Figure 4. Percent transmittance (%T) for P(2VP/NaSS)$_n$ at various pH values in water (open blue triangle) and in the NaCl aqueous solution (open red circle): (a) n = 19 and [NaCl] = 0.1 M and (b) n = 95 and [NaCl] = 1.2 M at 25 °C.

solution. Here, P(2VP/NaSS)$_{19}$ maintained a 100%T in a pH range of 3.4−10 in water. Following this, a sharp phase transition from a clear to a cloudy state occurred and, within a short pH range (=0.5), the %T reached 0%. From the intersection, the critical pH value was estimated to be 3.4. Meanwhile, in the NaCl aqueous solution, the critical pH value was estimated to be 3.1. At the critical pH value, the pyridine ring of the polymers was protonated, and electrostatic attraction occurred with the anionic sulfonate group, resulting in the solutions becoming cloudy. Salt can screen the charge of the ionic group. For P(2VP/NaSS)$_{19}$, the phase transition from a clear to cloudy state shifted to a lower pH value in the presence of NaCl because of the screening of the electrostatic attractions. For P(2VP/NaSS)$_{95}$, the %T remained at 100% in a pH range of 4.4−10 in water before the %T reached 0% within a narrow pH range (=0.5). In the presence of 1.2 M NaCl, a broad phase transition was observed at pH = 5.4. A relatively broad pH range (=2) was required for the %T to reach or approach 0% at pH = 3. Following this, the %T increased to 9% until pH = 2. For P(2VP/NaSS)$_{95}$, the critical pH value was estimated to be 4.4 and 5.4 in water and in the 1.2 M NaCl aqueous solution, respectively. These behaviors suggested that the protonated 2VP units interacted with the

NaSS units due to electrostatic and reversible hydrogen bonding interactions. Here, the phase transition occurred at a higher pH value in the presence of NaCl. This behavior differed from the normal phenomenon observed for P(2VP/NaSS)$_{19}$. In the experiment (Figure 4), the salt effect on P(2VP/NaSS)$_{19}$ was little because the additional NaCl concentration was low (0.1 M). On the other hand, the salt effect on P(2VP/NaSS)$_{95}$ was obviously observed because a large amount of NaCl was added (1.2 M). These observations suggested that it was related with the transformation from interchain interaction to intrachain interaction.[31,55]

Below the critical pH temperature, driven phase transition behavior for the aqueous P(2VP/NaSS)$_{19}$ solution was observed following a heating and cooling process at pH = 2 and [NaCl] = 0.15 M with C_p = 2 g/L. The temperature dependence of %T was measured to estimate the T_p (phase transition temperature). First, two consecutive heating and cooling cycles were performed (Figure S5). The intersection point of the two tangents was at %T = 100%, with any decrease from 100% taken as the T_p. The T_p values for the two heating cycles were 47.7 and 47.8 °C, whereas those for the cooling cycles were both 43.8 °C. The intersection point of the two tangents was at %T = 100%, with any decrease from 100% taken as the T_p. Although the T_p values for the heating and cooling cycles were consistent, they were different with a hysteresis of around 4 °C. During the cooling process, the polymer chains aggregated from a unimer state and the solution became cloudy, whereas during the heating process, the aggregated polymers shifted to a unimer state and the solution thus became clear. In this case, any entangled polymer chains dissociated from the unimer state and became kinetically unfavorable compared with the opposite phase transition from unimer to aggregate. Moreover, the phase transition during the heating cycle was somewhat broader than that during the cooling cycle. Therefore, in this study, we focused on the cooling process of the phase transition.
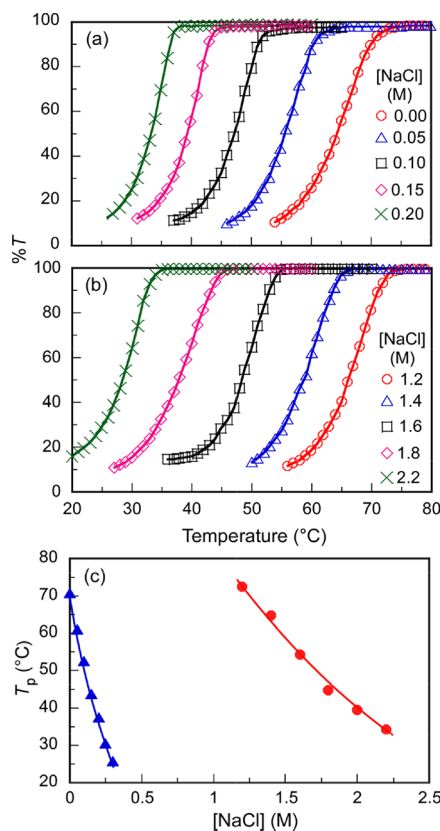
To estimate the T_p values for the aqueous P(2VP/NaSS)$_{19}$ solutions, the %T values were measured as a function of temperature at different pH values ranging from 1.9 to 2.6 at [NaCl] = 0.1 M with C_p = 2 g/L during the cooling process (Figure 5a). Here, the T_p values decreased with an increase in pH value. For example, the T_p value at pH = 1.9 was found to be 56.1 °C, whereas at pH = 2.6, the value was calculated to be 31.9 °C at [NaCl] = 0.1 M. The T_p values for the aqueous P(2VP/NaSS)$_{95}$ solutions were measured according to %T as a function of temperature during the cooling process under various pH conditions ranging from 2.0 to 3.8 at [NaCl] = 1.2 M with C_p = 2 g/L (Figure 5b). Here, the T_p shifted to lower values when the pH value was increased. For the aqueous P(2VP/NaSS)$_{95}$ solutions, the T_p values at pH 2.0 and 3.8 were observed to be 72.5 and 34.7 °C, respectively. At a lower pH value, 2VP was protonated and, because of the strong electrostatic interactions with the anionic NaSS, intra- and interpolymer aggregates were formed, with the T_p shifting to higher values. However, with an increase in pH value, deprotonation occurred and weakened the interactions. Therefore, at higher pH values, the T_p shifted to lower temperatures. As shown in Figure 5c, at the same pH value, the T_p for P(2VP/NaSS)$_{19}$ was lower than that for P(2VP/NaSS)$_{95}$. Moreover, the T_p values changed within a narrower pH range with P(2VP/NaSS)$_{19}$ than with P(2VP/NaSS)$_{95}$. These findings suggest that polymers with lower molecular
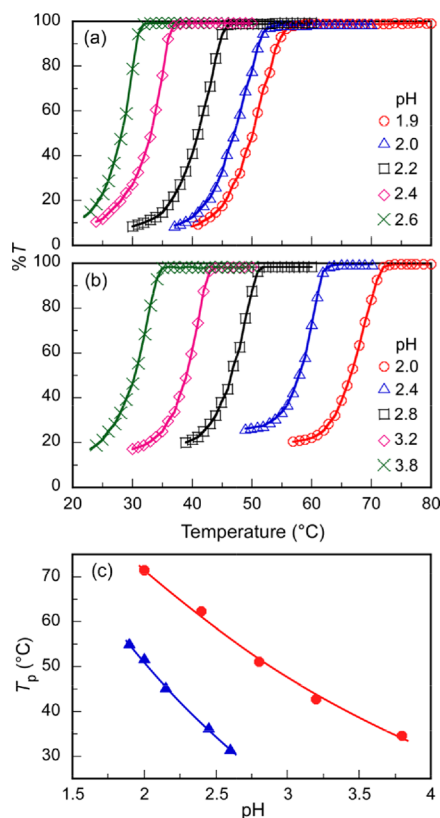
Figure 5. %T at 700 nm for the aqueous solutions of (a) P(2VP/NaSS)$_{19}$ at [NaCl] = 0.1 M and (b) P(2VP/NaSS)$_{95}$ at [NaCl] = 1.2 M with C_p = 2 g/L as a function of temperatures at varying pH values during the cooling processes. (c) pH dependence on the T_p for the aqueous solutions of P(2VP/NaSS)$_{19}$ (solid blue triangle) at [NaCl] = 0.1 M and P(2VP/NaSS)$_{95}$ (solid red circle) at [NaCl] = 1.2 M with C_p = 2 g/L.

Figure 6. Percent transmittance (%T) at 700 nm for the aqueous solutions of (a) P(2VP/NaSS)$_{19}$ and (b) P(2VP/NaSS)$_{95}$ with C_p = 2 g/L at pH = 2 as a function of temperatures at varying [NaCl] during the cooling processes. (c) [NaCl] dependence on the T_p for the aqueous solutions of P(2VP/NaSS)$_{19}$ (solid blue triangle) and P(2VP/NaSS)$_{95}$ (solid red circle) with C_p = 2 g/L at pH = 2.

weight are more sensitive to a change in conditions than those with a higher molecular weight.

We studied the [NaCl] dependence on the T_p value of the aqueous P(2VP/NaSS)$_{19}$ solutions using the %T measurements as a function of temperature at pH = 2 with C_p = 2 g/L (Figure 6a). Here, the T_p shifted to lower values with an increase in [NaCl], with the T_p values of the aqueous P(2VP/NaSS)$_{19}$ solution at [NaCl] = 0.05 and 0.2 M found to be 61.0 and 37.6 °C, respectively. The temperature dependence on the %T was measured for the aqueous P(2VP/NaSS)$_{95}$ solution at various [NaCl] at pH = 2 with C_p = 2 g/L (Figure 6b). Here, the T_p values decreased with an increase in [NaCl], with the T_p values of the aqueous P(2VP/NaSS)$_{95}$ solution at [NaCl] = 1.2 and 2.2 M found to be 72.5 and 34.2 °C, respectively, at pH = 2 with C_p = 2 g/L. At a low salt concentration, the Coulombic interactions among the polymer units tend to be high. However, added salt can screen the charges of the ionic group. Therefore, at high [NaCl] values, the interactions among the polymer chains will be weakened, and the polymer could dissolve at a relatively low temperature, thus decreasing the T_p value. We thus measured the T_p for the aqueous P(2VP/NaSS)$_{19}$ and P(2VP/NaSS)$_{95}$ solutions. Here, the aqueous P(2VP/NaSS)$_{19}$ solution exhibited a phase transition at 70.8 °C and at pH = 2 with C_p = 2 g/L. However, the aqueous P(2VP/NaSS)$_{95}$ solution did not exhibit any phase transition at pH = 2 with C_p = 2 g/L. Heat was applied to dissolve the polymer up to the boiling point of water. However,
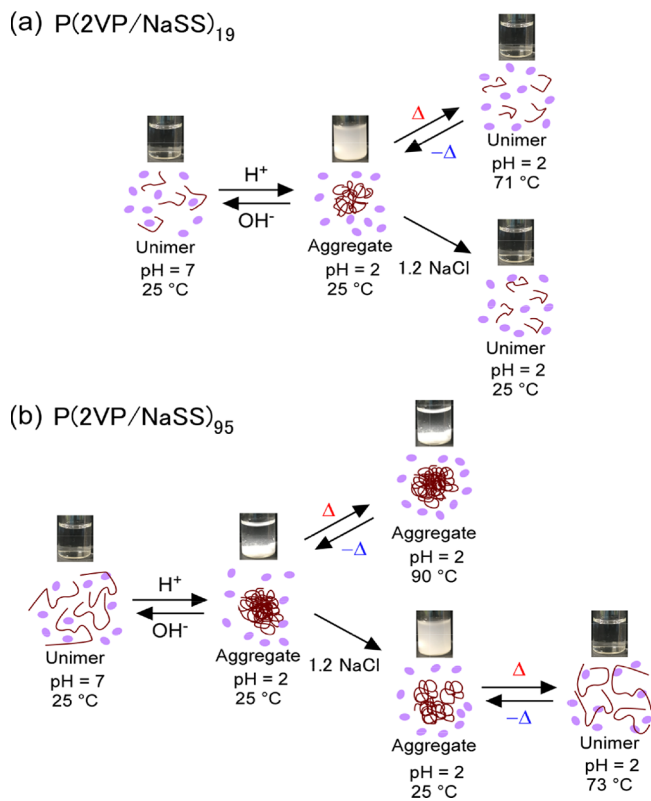
the polymer remained precipitated throughout the temperature range (Scheme 2), which will be further discussed later. As shown in Figure 6c, the T_p of P(2VP/NaSS)$_{19}$ changed within a narrower [NaCl] range than that of P(2VP/NaSS)$_{95}$. This suggests that polymers with a lower molecular weight are more sensitive to [NaCl] than those with a higher molecular weight.

The effect of the C_p on the T_p of the P(2VP/NaSS)$_{19}$ aqueous solution obtained via the %T measurement as a function of temperature at pH = 2 with [NaCl] = 0.1 M was studied at a range of 0.5−4 g/L (Figure 7a). Meanwhile, the %T of the aqueous P(2VP/NaSS)$_{95}$ solution was measured as a function of temperature at a C_p range of 0.5−2.2 g/L at pH = 2 and [NaCl] = 1.2 M (Figure 7b). At high C_p values, strong interactions among the polymer chains occurred because of the increasing entanglement of the polymer chains. Consequently, a great deal of energy will be needed to weaken the interactions among the polymer chains with high C_p values. Thus, the T_p value shifted to a higher temperature at high C_p values. Here, the T_p of P(2VP/NaSS)$_{95}$ was higher than that of P(2VP/NaSS)$_{19}$ at the same C_p value (Figure 7c). With an increase in chain length, the interactions among the polymer chains will tend to occur more easily. Hence, the polymer chains will aggregate easier in P(2VP/NaSS)$_{95}$ because of its higher molecular weight than in (2VP/NaSS)$_{19}$, with a consequential increase in T_p.

The polymers with C_p = 2.0 g/L could dissolve in pure water at pH = 7 and 25 °C as a unimer state. At pH = 2 and 25 °C, the aqueous P(2VP/NaSS)$_{19}$ solution became cloudy (Scheme

Scheme 2. Solution Behaviors of (a) P(2VP/NaSS)$_{19}$ and (b) P(2VP/NaSS)$_{95}$ under Acidic and Basic Conditions in the Absence and Presence of NaCl Above and Below the UCST

(a) P(2VP/NaSS)$_{19}$

(b) P(2VP/NaSS)$_{95}$

Figure 7. Percent transmittance (%T) at 700 nm for the aqueous solutions of (a) P(2VP/NaSS)$_{19}$ at [NaCl] = 0.1 M and (b) P(2VP/NaSS)$_{95}$ at [NaCl] = 1.2 M and pH = 2 as a function of temperature at varying C_p in the cooling processes. (c) C_p dependence on the T_p for the aqueous solutions of P(2VP/NaSS)$_{19}$ (solid blue triangle) at [NaCl] = 0.1 M and P(2VP/NaSS)$_{95}$ (solid red circle) at [NaCl] = 1.2 M and pH = 2.

2a), whereas at 71 °C, the solution became as clear as before, and upon cooling to 25 °C, it regained its cloudy dispersion. However, when 1.2 M NaCl was added to the polymer solution at pH = 2 and 25 °C, the solution became clear. At 25 °C, the polymer dissolved in pure water as a unimer state because of the repulsion among the sulfonate anions, with a zeta potential of −1.5 mV. The pendant pyridine rings in the 2VP units were protonated when the pH value decreased to 2. Thus, the solution became cloudy following the occurrence of strong intra- and interpolymer electrostatic attractive interactions with the anionic sulfone and cationic protonated pyridine groups. The interpolymer interactions of P(2VP/NaSS)$_{19}$ with a short chain length were weaker than those of P(2VP/NaSS)$_{95}$ with a long chain length. Meanwhile, the aqueous P(2VP/NaSS)$_{19}$ solution became cloudy at pH = 2 and 25 °C. At 71 °C, P(2VP/NaSS)$_{19}$ dissolved in water at pH = 2 as a unimer state since the molecular motion increased to weaken the electrostatic interactions. When 1.2 M NaCl was added to the P(2VP/NaSS)$_{19}$ solution at pH = 2 and 25 °C, the charge interactions were fully screened for dissolving in the aqueous solution as a unimer state. For the aqueous P(2VP/NaSS)$_{95}$ solution, the polymer dissolved in pure water at pH = 7 and 25 °C as a unimer state; however, at pH = 2, the polymer was precipitated out of the solution (Scheme 2b). At pH = 2 and 25 °C, the P(2VP/NaSS)$_{95}$ solution precipitated to form a large aggregate due to the intra- and interpolymer electrostatic interactions because the pendant pyridine rings in the 2VP unit were protonated to generate cationic charges that interacted with the anionic sulfonate anions. P(2VP/NaSS)$_{95}$ with a long polymer chain facilitated the entanglement among
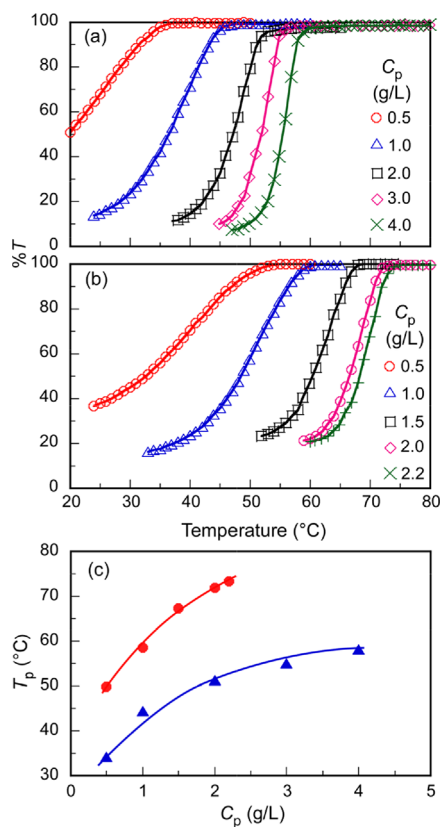
the polymer chains, which led to the formation of a large aggregate with consequential precipitation of the aggregates from the solution. Up to 90 °C, the aggregate could not be dissolved because of the strong electrostatic interactions. The addition of 1.2 M NaCl made the solution turn cloudy, whereas when heat was applied at 73 °C, the solution returned to a clear state. At pH = 7 and 25 °C, P(2VP/NaSS)$_{95}$ dissolved in the aqueous solution as a unimer state because of the electrostatic repulsions of the pendant sulfonate anions, with the a zeta potential of −2.15 mV. At pH = 2 and 73 °C, the molecular motion of P(2VP/NaSS)$_{95}$ overcame the electrostatic attractive interactions to allow for dissolution in the aqueous solution as a unimer state.

DLS measurements were performed to obtain the R_h (hydrodynamic radius) values and the distribution data for the copolymers (Figure S6). For the P(2VP/NaSS)$_{19}$ aqueous solution, measurements were performed above and below the UCST at [NaCl] = 0.2 M and pH = 2 with C_p = 2.0 g/L. Here, the R_h distributions were unimodal, with those above and below the UCST being 1.8 and 1268 nm, respectively. For the P(2VP/NaSS)$_{95}$ aqueous solution, measurements were performed above and below the UCST at [NaCl] = 2.2 M and pH = 2 with C_p = 2.0 g/L. Here, unimodal R_h distributions were obtained, with those above and below the T_p being 2.9 and 2591 nm, respectively. The small and large values above and below the T_p indicate the unimer and aggregation state of the polymers.

The UCST behavior was investigated in terms of the temperature dependence on the light scattering and DLS measurements (Figure S7). The R_h and SI (scattering intensity) values for the aqueous $P(2VP/NaSS)_n$ solutions were measured as a function of temperature in the cooling processes. Here, the T_p was determined as a point where the R_h and SI suddenly increased with a decrease in temperature. The R_h values of $P(2VP/NaSS)_{19}$ and $P(2VP/NaSS)_{95}$ remained almost constant as small values above the T_p, whereas the respective SI values remained small above the T_p. These small R_h and SI values suggest that $P(2VP/NaSS)_n$ had a unimer state above the T_p. Meanwhile, below the T_p, large aggregates were formed, and the solutions became cloudy. The T_p values obtained via the light scattering measurements were in good agreement with the results of the %T measurements. For example, the T_p for $P(2VP/NaSS)_{19}$ at [NaCl] = 0.2 M and pH = 2 with C_p = 2.0 g/L was estimated to be 37.6 °C in the R_h and SI measurements, whereas it was estimated to be 36.9 °C in the %T measurements.

The T_p value of the aqueous $P(2VP/NaSS)_n$ solution was also affected by isotopes (Figure 8). The effect of isotopes on
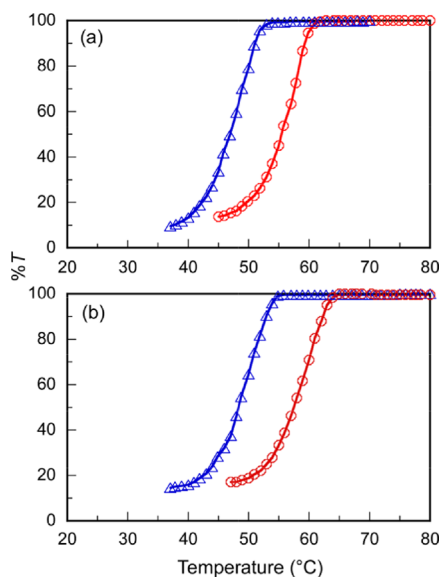
Figure 8. %T at 700 nm for the H_2O (open blue triangle) and D_2O (open red circle) solutions of (a) $P(2VP/NaSS)_{19}$ at [NaCl] = 0.1 M and (b) $P(2VP/NaSS)_{95}$ at [NaCl] = 1.2 M and pH = 2 with C_p = 2 g/L as a function of temperature.

the T_p of LCST and UCST polymers has been studied by various research groups.[56−58] Here, the T_p value of $P(2VP/NaSS)_n$ was found to be higher in D_2O than in H_2O, with the T_p values of $P(2VP/NaSS)_{19}$ copolymers being 60.4 and 52.1 °C in D_2O and H_2O, respectively, at pH = 2 and [NaCl] = 0.1 M with C_p = 2 g/L. Meanwhile, the T_p values of $P(2VP/NaSS)_{95}$ were 63.4 and 54.2 °C in D_2O and H_2O, respectively, at pH = 2 and [NaCl] = 1.6 M with C_p = 2 g/L. Since deuterium is heavier than hydrogen, the amplitude of atomic vibration is lower in D_2O than in H_2O,[59] which also facilitates the D_2O molecules to be structurally more organized than those in H_2O.[60] In polymer solutions, there is a hydration layer around the polymer, which is commonly known as hydrophobic hydration. The hydration layer formed by D_2O is structurally more stable than that formed by H_2O molecules. Because of the high stability of the hydration layer formed by

D_2O, it seeks more energy than H_2O to break the layer, with a consequential increase in T_p value.

CONCLUSIONS

The controlled synthesis of statistical copolymers, $P(2VP/NaSS)_n$ with n = 19 and 95, was achieved via the copolymerization of 2VP and NaSS using the RAFT technique. The time conversion plot, monomer reactivity ratios, ^1H NMR DOSY, and UV−vis absorption measurements suggested that $P(2VP/NaSS)_n$ is a close to ideal random copolymer with a slightly higher molar content of the 2VP unit. Under acidic conditions, the protonated 2VP units interacted with the anionic NaSS units. $P(2VP/NaSS)_n$ exhibited temperature-mediated phase transition behavior because of the charge interactions. The T_p values for the aqueous $P(2VP/NaSS)_n$ solutions increased with an increase in pH, C_p, and molecular weight and with a reduction in [NaCl]. Therefore, the T_p value can be modulated via the appropriate adjustment of these factors. The deuterium isotope also affected the T_p value, which was higher in D_2O than in H_2O. Thus, a tailorable T_p will facilitate the application of the copolymers in various fields.

EXPERIMENTAL SECTION

Materials. Sodium *p*-styrenesulfonate (NaSS, 98%) and 4,4′-azobis(4-cyanopentanoic acid) (V-501, 98%) were purchased from Fujifilm Wako Pure Chemical Industries, Ltd. (Osaka, Japan) and used without further purification. Meanwhile, 2-vinylpyridine (2VP, 97%) was purchased from the same company and was distilled under reduced pressure after drying with 3 Å molecular sieves, whereas 4-cyanopentanoic acid dithiobenzoate (CPD) was prepared according to a previously reported method.[61] Methanol (MeOH) was distilled following drying using 3 Å molecular sieves, whereas water was purified using an ion exchange column system. All other reagents were used as received.

Monomer Reactivity Ratios. The monomer reactivity ratios of 2VP and NaSS were determined using the following method. 2VP was dissolved in a D_2O/methanol-d_4 (7/3; v/v) mixed solvent before NaSS was added with a feed ratio of 10−90 mol %. An initiator, V-501, was then added to the solution, ([2VP] + [NaSS])/[V-501] = 100/0.5, whereas 1,4-dioxane was used as an internal standard for the nuclear magnetic resonance (NMR) measurements. The pH of the solution was recorded to be 6.88. Then, the solutions were purged with argon gas, and polymerization was conducted at 70 °C below 15% of the monomer conversion. The content of 2VP in the copolymer was estimated from the conversion of 2VP evaluated by ^1H NMR analysis.

^1H NMR Diffusion-Ordered Spectroscopy. Self-diffusion of monomers and their complexes is different. ^1H NMR diffusion-ordered spectroscopy (DOSY) measurements were performed to understand the interactions between the monomers. The measurements were conducted using a JEOL (Tokyo, Japan) JNM-ECZ 400 spectrometer, with the diffusion-ordered spectra acquired at 25 °C. Analysis was conducted using Delta 5.3.1 software to obtain 1D or 2D data.

Preparation of $P(2VP/NaSS)_n$. To study the relationship between the polymerization time and the conversion of equimolar amounts of 2VP and NaSS via RAFT polymerization, the following method was used. Samples of 2VP (105 mg, 1.00 mmol), NaSS (206 mg, 1.00 mmol), CPD (27.9 mg,

0.10 mmol), and V-501 (14.0 mg, 0.05 mmol) were dissolved in a mixed solvent of D_2O (1.8 mL) and methanol-d_4 (0.2 mL) ([2VP]/[NaSS]/[CPD]/[V-501] = 10/10/1/0.5; molar ratio). The solution pH was 6.77. To obtain NMR data at regular intervals, polymerization was conducted at 70 °C under an Ar atmosphere using NMR equipment. Conversion was estimated from the integral intensity of the vinyl protons observed at 4.9−6.0 ppm in relation to the peak of the internal standard at 3.7 ppm.

P(2VP/NaSS)$_n$ samples were prepared via RAFT polymerization (Scheme S1). In terms of the preparation method for P(2VP/NaSS)$_{19}$, 2VP (262.8 mg, 2.5 mmol), NaSS (515.7 mg, 2.5 mmol), CPD (69.9 mg, 0.25 mmol), and V-501 (35.9 mg, 0.13 mmol) were dissolved in a mixed solvent of water (4.5 mL) and MeOH (0.5 mL) ([2VP]/[NaSS]/[CPD]/[V-501] = 10/10/1/0.5; molar ratio) before the solution was heated at 71 °C for 14 h under an Ar atmosphere. The pH of the polymerization solution was 6.35. Following polymerization, the total monomer conversion, estimated from the ^1H NMR data, was 94.1%. The reaction mixture was initially dialyzed against methanol for 16 h and then against pure water for 24 h. P(2VP/NaSS)$_{19}$ was recovered using a freeze-drying method (565 mg, 74.6%). The theoretical DP and number-average molecular weight (M_n) were calculated as 19 and 2.97×10^3 g/mol, respectively. The same method was also used to prepare P(2VP/NaSS)$_{95}$ (1.30 g, 83.2%).

Measurements. Both ^1H and ^{13}C NMR spectra were obtained using a JEOL (Tokyo, Japan) JNM-ECZ 400 spectrometer, whereas infrared (IR) spectroscopic measurements were performed on a Jasco (Tokyo, Japan) FT/IR-4200 using the attenuated total reflection (ATR) technique. The incident angle applied for the sample was 45°. The samples were measured using 256 scans, with Jasco Spectra Manager Version 2 software used to analyze the spectra. The phase separation temperatures of the polymer aqueous solutions were measured in terms of percent transmittance (%T) with a 700 nm light beam exerted through a quartz sample cell with a 10 mm path length. The %T was recorded using a Jasco (Tokyo, Japan) V-630BIO UV−vis spectrophotometer equipped with a Jasco ETC-717 temperature controller system, with the temperature controlled using an Eyela (Tokyo, Japan) NCB-1200 thermostatted water bath. The temperature was increased from 20 to 80 °C and then reduced from 80 back to 20 °C, with a heating and cooling rate of 1.0 °C/min. The absorption spectra of the monomer aqueous solutions were measured via a 190−350 nm light beam using the same UV−vis spectrophotometer at 25 °C. Dynamic light scattering (DLS) measurements were conducted using a Malvern (Malvern, UK) Zetasizer Nano-ZS instrument equipped with a He−Ne laser at 20−45 °C. The laser operates at λ = 632.8 nm, whereas the scattering angle was fixed at 173°. For the DLS measurements, all the sample solutions were filtered with a 0.2 μm pore size filter, with the obtained data analyzed using Malvern (Malvern, UK) Zetasizer Software 7.11. The SI and R_h used in this study are the average value of three measurements. The T_p based on the R_h and SI was determined during a cooling process where the temperature was reduced from 50 to 20 °C with a cooling rate of 0.3 °C/min. During the phase transition, the temperature measurement samples were filtered with a 0.2 μm pore size filter placed above the UCST of the respective sample.

■ ASSOCIATED CONTENT

ⓢ Supporting Information

The Supporting Information is available free of charge at https://pubs.acs.org/doi/10.1021/acsomega.1c00351.

Synthesis scheme of P(2VP/NaSS)$_n$; 2D DOSY NMR spectra of NaSS and equimolar mixture of NaSS and 2VP in D_2O at 25 °C; UV−vis absorption spectra of 2VP and NaSS and equimolar mixture of both monomers at 25 °C in pure water; ATR-IR spectra of P(2VP/NaSS)$_{19}$ and P(2VP/NaSS)$_{95}$; ^1H NMR spectra for P(2VP/NaSS)$_{19}$ and P(2VP/NaSS)$_{95}$ in D_2O at 25 °C; percent transmittance (%T) at 700 nm for P(2VP/NaSS)$_{19}$ as a function of temperature over two heating and cooling cycles; hydrodynamic radius (R_h) distributions of P(2VP/NaSS)$_{19}$ and P(2VP/NaSS)$_{95}$ aqueous solutions at 25 °C and 40 °C; and hydrodynamic radius (R_h) and light SI of P(2VP/NaSS)$_{19}$ and P(2VP/NaSS)$_{95}$ aqueous solutions as a function of temperature (PDF)

■ AUTHOR INFORMATION

Corresponding Author

Shin-ichi Yusa − Department of Applied Chemistry, Graduate School of Engineering, University of Hyogo, Himeji, Hyogo 671-2280, Japan; ⊙ orcid.org/0000-0002-2838-5200; Email: yusa@eng.u-hyogo.ac.jp

Authors

Komol Kanta Sharker − Department of Applied Chemistry, Graduate School of Engineering, University of Hyogo, Himeji, Hyogo 671-2280, Japan

Yusuke Shigeta − Tosoh Finechem Co., Shunan, Yamaguchi 746-0006, Japan

Shinji Ozoe − Tosoh Finechem Co., Shunan, Yamaguchi 746-0006, Japan

Panittha Damsongsang − Department of Chemistry, Faculty of Science, Chulalongkorn University, Bangkok 10330, Thailand

Voravee P. Hoven − Department of Chemistry, Faculty of Science, Chulalongkorn University, Bangkok 10330, Thailand; ⊙ orcid.org/0000-0002-1330-6784

Complete contact information is available at:
https://pubs.acs.org/10.1021/acsomega.1c00351

Notes

The authors declare no competing financial interest.

■ ACKNOWLEDGMENTS

■ REFERENCES

(1) Teotia, A.K.; Sami, A.; Kumar, H. Thermo-responsive polymers. In *Switchable and Responsive Surfaces and Materials for Biomedical Applications; Woodhead Publishing*; Elsevier: 2015; pp. 3−43.

(2) Dai, S.; Ravi, P.; Tam, K. C. pH-Responsive Polymers: Synthesis, Properties and Applications. *Soft Matter* **2008**, *4*, 435−449.

(3) García, M. C. 14-Ionic-Strength-Responsive Polymers for Drug Delivery Applications. In *Stimuli Responsive Polymeric Nanocarriers for Drug Delivery Applications*, Vol. 2, Woodhead Publishing; Elsevier: 2019, pp. 393−409.

(4) Bertrand, O.; Gohy, J. F. Photo-Responsive Polymers: Synthesis and Applications. *Polym. Chem.* **2017**, *8*, 52−73.

(5) Tanaka, T.; Nishio, I.; Sun, S.-T.; Ueno-Nishio, S. Collapse of Gels in an Electric Field. *Science* **1982**, *218*, 467−469.

(6) Thévenot, J.; Oliveira, H.; Sandre, O.; Lecommandoux, S. Magnetic Responsive Polymer Composite Materials. *Chem. Soc. Rev.* **2013**, *42*, 7099−7116.

(7) Ma, G.; Lin, W.; Yuan, Z.; Wu, J.; Qian, H.; Xu, L.; Chen, S. Development of Ionic Strength/pH/Enzyme Triple-Responsive Zwitterionic Hydrogel of the Mixed l-Glutamic Acid and l-Lysine Polypeptide for Site-Specific Drug Delivery. *J. Mater. Chem. B* **2017**, *5*, 935−943.

(8) Zhang, Z.; Wang, J.; Nie, X.; Wen, T.; Ji, Y.; Wu, X.; Zhao, Y.; Chen, C. Near Infrared Laser-Induced Targeted Cancer Therapy Using ThermoResponsive Polymer Encapsulated Gold Nanorods. *J. Am. Chem. Soc.* **2014**, *136*, 7317−7326.

(9) Gupta, M. K.; Martin, J. R.; Werfel, T. A.; Shen, T.; Page, J. M.; Duvall, C. L. Cell Protective, ABC Triblock Polymer-Based ThermoResponsive Hydrogels with Ros-Triggered Degradation and Drug Release. *J. Am. Chem. Soc.* **2014**, *136*, 14896−14902.

(10) Twaites, B. R.; de Las Heras Alarcón, C.; Lavigne, M.; Saulnier, A.; Pennadam, S. S.; Cunliffe, D.; Górecki, D. C.; Alexander, C. Thermoresponsive Polymers as Gene Delivery Vectors: Cell Viability, DNA Transport and Transfection Studies. *J. Controlled Release* **2005**, *108*, 472−483.

(11) Shamim, N.; Hong, L.; Hidajat, K.; Uddin, M. S. ThermoSensitive Polymer Coated Nanomagnetic Particles for Separation of Bio-Molecules. *Sep. Purif. Technol.* **2007**, *53*, 164−170.

(12) Reese, C. E.; Mikhonin, A. V.; Kamenjicki, M.; Tikhonov, A.; Asher, S. A. Nanogel Nanosecond Photonic Crystal Optical Switching. *J. Am. Chem. Soc.* **2004**, *126*, 1493−1496.

(13) Wu, W.; Zhou, T.; Berliner, A.; Banerjee, P.; Zhou, S. Smart Core-Shell Hybrid Nanogels with Ag Nanoparticle Core for Cancer Cell Imaging and Gel Shell for pH-Regulated Drug Delivery. *Chem. Mater.* **2010**, *22*, 1966−1976.

(14) Wang, B.; Liu, H. J.; Jiang, T. T.; Li, Q. H.; Chen, Y. Thermo-, and pH Dual-Responsive Poly(*N*-vinylimidazole): Preparation, Characterization and Its Switchable Catalytic Activity. *Polymer* **2014**, *55*, 6036−6043.

(15) Debord, J. D.; Lyon, L. A. Synthesis and Characterization of pH-Responsive Copolymer Microgels with Tunable Volume Phase Transition Temperatures. *Langmuir* **2003**, *19*, 7662−7664.

(16) Serpe, M. J.; Lyon, L. A. Optical and Acoustic Studies of pH-Dependent Swelling in Microgel Thin Films. *Chem. Mater.* **2004**, *16*, 4373−4380.

(17) Kocak, G.; Tuncer, C.; Bütün, V. pH-Responsive Polymers. *Polym. Chem.* **2017**, *8*, 144−176.

(18) Kudaibergenov, S. E.; Ciferri, A. Natural and Synthetic Polyampholytes, 2. *Macromol. Rapid Commun.* **2007**, *28*, 1969−1986.

(19) Heskins, M.; Guillet, J. E. Solution Properties of Poly(*N*-isopropylacrylamide). *J. Macromol. Sci., Chem.* **1968**, *2*, 1441−1455.

(20) Roy, D.; Brooks, W. L. A.; Sumerlin, B. S. New Directions in ThermoResponsive Polymers. *Chem. Soc. Rev.* **2013**, *42*, 7214−7243.

(21) Weber, C.; Hoogenboom, R.; Schubert, U. S. Temperature Responsive Bio-Compatible Polymers Based on Poly(ethylene oxide) and Poly(2-oxazoline)s. *Prog. Polym. Sci.* **2012**, *37*, 686−714.

(22) Kjøniksen, A.-L.; Laukkanen, A.; Galant, C.; Knudsen, K. D.; Tenhu, H.; Nyström, B. Association in Aqueous Solutions of a ThermoResponsive PVCL-*g*-C₁₁EO₄₂copolymer. *Macromolecules* **2005**, *38*, 948−960.

(23) Vancoillie, G.; Frank, D.; Hoogenboom, R. ThermoResponsive Poly(oligo ethylene glycol acrylates). *Prog. Polym. Sci.* **2014**, *39*, 1074−1095.

(24) Song, Z.; Wang, K.; Gao, C.; Wang, S.; Zhang, W. A New Thermo-, pH-, and CO₂-Responsive Homopolymer of Poly[*N*-[2-(diethylamino)ethyl]acrylamide]: Is the Diethylamino Group Underestimated? *Macromolecules* **2016**, *49*, 162−171.

(25) Karjalainen, E.; Aseyev, V.; Tenhu, H. Influence of Hydrophobic Anion on Solution Properties of PDMAEMA. *Macromolecules* **2014**, *47*, 2103−2111.

(26) Zhang, Q.; Hoogenboom, R. UCST Behavior of Polyampholytes Based on Stoichiometric RAFT Copolymerization of Cationic and Anionic Monomers. *Chem. Commun.* **2015**, *51*, 70−73.

(27) Laschewsky, A. Structures and Synthesis of Zwitterionic Polymers. *Polymer* **2014**, *6*, 1544−1601.

(28) Klenina, O. V.; Fain, E. G. Phase Separation in the System Polyacrylic Acid-Polycrylamide-Water. *Polym. Sci. U.S.S.R.* **1981**, *23*, 1439−1446.

(29) Ohnishi, N; Aoshima, K; Kataoka, K; Ueno, K. *Agency of Industrial Science and Technology MITI*; Japan Chemical Innovation Institute, E.P. **1999**, *0*, 715 A2.

(30) Seuring, J.; Agarwal, S. Non-Ionic Homo- and Copolymers with H-Donor and H-Acceptor Units with an UCST in Water. *Macromol. Chem. Phys.* **2010**, *211*, 2109−2117.

(31) Schulz, D. N.; Peiffer, D. G.; Agarwal, P. K.; Larabee, J.; Kaladas, J. J.; Soni, L.; Handwerker, B.; Garner, R. T. Phase Behaviour and Solution Properties of Sulphobetaine Polymers. *Polymer* **1986**, *27*, 1734−1742.

(32) Sharker, K. K.; Ohara, Y.; Shigeta, Y.; Ozoe, S.; Yusa, S.-i. Upper Critical Solution Temperature (UCST) Behavior of Polystyrene-Based Polyampholytes in Aqueous Solution. *Polymer* **2019**, *11*, 265−277.

(33) Li, Z.; Hao, B.; Tang, Y.; Li, H.; Lee, T. C.; Feng, A.; Zhang, L.; Thang, S. H. Effect of End-groups on Sulfobetaine Homopolymers with the Tunable Upper Critical Solution Temperature (UCST). *Eur. Polym. J.* **2020**, *132*, 109704−109713.

(34) Zhu, Y.; Noy, J.-M.; Lowe, A. B.; Roth, P. J. The Synthesis and Aqueous Solution Properties of Sulfobutylbetaine (co)polymers: Comparison of Synthetic Routes and Tuneable Upper Critical Solution Temperatures. *Polym. Chem.* **2015**, *6*, 5705−5718.

(35) Vasantha, V. A.; Jana, S.; Parthiban, A.; Vancso, J. G. Water Swelling, Brine Soluble Imidazole Based Zwitterionic Polymers—Synthesis and Study of Reversible UCST Behaviour and Gel−Sol Transitions. *Chem. Commun.* **2014**, *50*, 46−48.

(36) Seuring, J.; Agarwal, S. First Example of a Universal and Cost-Effective Approach: Polymers with Tunable Upper Critical Solution Temperature in Water and Electrolyte Solution. *Macromolecules* **2012**, *45*, 3910−3918.

(37) Pineda-Contreras, B. A.; Liu, F.; Agarwal, S. Importance of Compositional Homogeneity of Macromolecular Chains for UCST-Type Transitions in Water: Controlled Versus Conventional Radical Polymerization. *J. Polym. Sci. Part A Polym. Chem.* **2014**, *52*, 1878−1884.

(38) Seuring, J.; Bayer, F. M.; Huber, K.; Agarwal, S. Upper Critical Solution Temperature of Poly(*N*-acryloyl glycinamide) in Water: A Concealed Property. *Macromolecules* **2012**, *45*, 374−384.

(39) Grubbs, R. B.; Grubbs, R. H. 50th Anniversary Perspective: Living Polymerization—Emphasizing the Molecule in Macromolecules. *Macromolecules* **2017**, *50*, 6979−6997.

(40) Marić, M.; Zhang, C.; Gromadzki, D. Poly(methacrylic acid-*ran*-2-vinylpyridine) Statistical Copolymer and Derived Dual pH-Temperature Responsive Block Copolymers by Nitroxide-Mediated Polymerization. *Processes* **2017**, *5*, 7−21.

(41) Varoqui, R.; Tran, Q.; Pefferkorn, E. Polycation-Polyanion Complexes in the Linear Diblock Copolymer of Poly(styrene sulfonate)/Poly(2-vinylpyridinium) Salt. *Macromolecules* **1979**, *12*, 831−835.

(42) Li, G.; Xu, N.; Yu, Q.; Lu, X.; Chen, H.; Cai, Y. Acceleration and Selective Monomer Addition during Aqueous RAFT Copolymerization of Ionic Monomers at 25 °C. *Macromol. Rapid Commun.* **2014**, *35*, 1430−1435.

(43) Wang, L.; Ding, Y.; Liu, Q.; Zhao, Q.; Dai, X.; Lu, X.; Cai, Y. Sequence-Controlled Polymerization-Induced Self-Assembly. *ACS Macro Lett.* **2019**, *8*, 623−628.

(44) Corpart, J. M.; Candau, F. Aqueous Solution Properties of Ampholytic Copolymers Prepared in Microemulsions. *Macromolecules* **1993**, *26*, 1333−1343.

(45) Yang, J. H.; John, M. S. The Conformation and Dynamics Study of Amphoteric Copolymers, P(sodium 2-methacryloyloxyethanesulfonate-*co*-2-methacryloyloxyethyltrimethylammonium iodide), Using Viscometry, ^{14}N-, and ^{23}Na-NMR. *J. Polym. Sci. A* **1995**, *33*, 2613−2621.

(46) O'Driscoll, K. F.; Reilly, P. M. Determination of Reactivity Ratios in Copolymerization. *Makromol. Chem. Macromol. Symp.* **1987**, *10-11*, 355−374.

(47) Cummings, S.; Zhang, Y.; Kazemi, N.; Penlidis, A.; Dubé, M. A. Determination of Reactivity Ratios for the Copolymerization of Poly(acrylic acid-*co*-itaconic acid). *J. Appl. Polym. Sci.* **2016**, *133*, 44014−44020.

(48) Fineman, M.; Ross, S. D. Linear Method for Determining Monomer Reactivity Ratios in Copolymerization. *J. Polym. Sci.* **1950**, *5*, 259−262.

(49) Odian, G. *Principles of Polymerization*; 3rd edition, John Wiley & Sons Inc.: New York, USA, 1995.

(50) Stevens, M. P. *Polymer Chemistry: An Introduction*; 3rd edition, Oxford University Press, New York: USA, 1999.

(51) Otsu, T.; Inoue, H. Alternative Copolymerizations of Vinyl Sulfides with Maleic Anhydride. *Makromol. Chem.* **1969**, *128*, 31−40.

(52) Salamone, J. C.; Tsai, C.-C.; Watterson, A. C. Polymerization of Vinylpyridinium Salts. XI. Charge-Transfer Polymerization of 4-Vinylpyridinium *p*-Styrenesulfonate. *J. Macromol. Sci. Chem.* **1979**, *13*, 665−672.

(53) Silverstein, R. M.; Bassler, G. C.; Morrill, T. C. *Spectrometric Identification of Organic Compounds*; 5th edition, John Wiley & Sons, Inc.: New York, USA, 1991.

(54) Seuring, J.; Agarwal, S. Polymers with Upper Critical Solution Temperature in Aqueous Solution. *Macromol. Rapid Commun.* **2012**, *33*, 1898−1920.

(55) Maji, T.; Banerjee, S.; Biswas, Y.; Mandal, T. K. Dual-Stimuli-Responsive L-Serine-Based Zwitterionic UCST-Type Polymer with Tunable Thermosensitivity. *Macromolecules* **2015**, *48*, 4957−4966.

(56) Endo, N.; Shirota, H.; Horie, K. Deuterium Isotope Effect on the Phase Separation of Zipper-type Hydrogen-Bonding Inter-Polymer Complexes in Solution. *Macromol. Rapid Commun.* **2001**, *22*, 593−597.

(57) Zhang, Y.; Furyk, S.; Bergbreiter, D. E.; Cremer, P. S. Specific Ion Effects on the Water Solubility of Macromolecules: PNIPAM and the Hofmeister Series. *J. Am. Chem. Soc.* **2005**, *127*, 14505−14510.

(58) Sun, W.; An, Z.; Wu, P. UCST or LCST? Composition Dependent Thermoresponsive Behavior of Poly(*N*-acryloylglycinamide-*co*-diacetone Acrylamide). *Macromolecules* **2017**, *50*, 2175−2182.

(59) Huff, A.; Patton, K.; Odhner, H.; Jacobs, D. T.; Clover, B. C.; Greer, S. C. Micellization and Phase Separation for Triblock Copolymer 17R4 in H_2O and in D_2O. *Langmuir* **2011**, *27*, 1707−1712.

(60) Luan, C. H.; Urry, D. W. Solvent Deuteration Enhancement of Hydrophobicity: DSC Study of the Inverse Temperature Transition of Elastin-Based Polypeptides. *J. Phys. Chem.* **1991**, *95*, 7896−7900.

(61) Yusa, S.; Yokoyama, Y.; Morishima, Y. Synthesis of Oppositely Charged Block Copolymers of Poly(ethylene glycol) via Reversible Addition−Fragmentation Chain Transfer Radical Polymerization and Characterization of Their Polyion Complex Micelles in Water. *Macromolecules* **2009**, *42*, 376−383.